

Connection of the stratospheric QBO with global atmospheric general circulation and tropical SST. Part II: interdecadal variations

Zeng-Zhen Hu · Bohua Huang · James L. Kinter III ·
Zhaohua Wu · Arun Kumar

Received: 15 April 2010 / Accepted: 5 April 2011 / Published online: 19 April 2011
© Springer-Verlag (outside the USA) 2011

Abstract The interdecadal variation of the association of the stratospheric quasi-biennial oscillation (QBO) with tropical sea surface temperature (SST) anomalies (SSTA) and with the general circulation in the troposphere and lower stratosphere is examined using the ERA40 and NCEP/NCAR reanalyses, as well as other observation-based analyses. It is found that the relationship between the QBO and tropical SSTA changed once around 1978–1980, and again in 1993–1995. During 1966–1974, negative correlation between the QBO and NINO3.4 indices reached its maximum when the NINO3.4 index lagged the QBO by less than 6 months. Correspondingly, the positive correlations were observed when the NINO3.4 index led the QBO by about 11–13 months or lagged by about 12–18 months. However, maximum negative correlations were shifted from the NINO3.4 index lagging the QBO by about 0–6 months during 1966–1974 to about 3–12 months during 1985–1992. During 1975–1979, both the negative and

positive correlations were relatively small and the QBO and ENSO were practically unrelated to each other. The phase-based QBO life cycle composites also confirm that, on average, there are two phase (6–7 months) delay in the evolution of the QBO-associated anomalous Walker circulation, tropical SST, atmospheric stability, and troposphere and lower stratosphere temperature anomalies during 1980–1994 in comparison with those in 1957–1978. The interdecadal variation of the association between the QBO and the troposphere variability may be largely due to the characteristic change of El Niño–Southern Oscillation. The irregularity of the QBO may play a secondary role in the interdecadal variation of the association.

Keywords Stratospheric QBO · Tropical Pacific SST · Interdecadal variation · Walker circulation · Tropical deep convection · ERA40 and NCEP/NCAR reanalyses · ENSO

Z.-Z. Hu (✉) · A. Kumar
Climate Prediction Center (Room 605), NCEP/NWS/NOAA,
5200 Auth Road, Camp Springs, MD 20746, USA
e-mail: Zeng-Zhen.Hu@noaa.gov

Z.-Z. Hu · B. Huang · J. L. Kinter III
Center for Ocean-Land-Atmosphere Studies, 4041 Powder Mill
Road, Suite 302, Calverton, MD 20705, USA

B. Huang · J. L. Kinter III
Department of Atmospheric, Oceanic, and Earth Sciences,
College of Science, George Mason University,
4400 University Drive, Fairfax, VA 22030, USA

Z. Wu
Department of Earth, Ocean, and Atmospheric Science,
and Center for Ocean-Atmospheric Prediction Studies,
Florida State University, 2035 E. Paul Dirac Drive,
Tallahassee, FL 32306, USA

1 Introduction

As discussed in Part I (Huang et al. 2011; hereafter HHKWK), there remain controversies about the stratospheric quasi-biennial oscillation (QBO) and its association with global climate variability. One of these controversies is how to isolate and represent the QBO signal and what is the phase evolution of the QBO life cycle. Another controversy is about the association of the QBO with tropical sea surface temperature (SST) anomalies (SSTA), especially those associated with El Niño and the Southern Oscillation (ENSO). HHKWK demonstrated that the Ensemble Empirical Mode Decomposition (EEMD) can successfully isolate the QBO time scale variability from the raw data. Using the QBO time scale component of zonal wind anomalies at 30 hPa (U30) isolated by EEMD to

represent the QBO, its life cycle composites of lower stratospheric and tropospheric variables, as well as SST, showed consistent results between the European Centre for Medium Range Weather Forecasts Re-Analysis (ERA40) and the National Centers for Environmental Prediction (NCEP)/National Center for Atmospheric Research (NCAR) reanalysis, as well as in situ radiosonde observations from Singapore. The results are also generally consistent with earlier investigations.

The analysis also demonstrated a statistically significant correlation between the QBO and tropical SSTA. On average, maximum negative correlations occur when the NINO3.4 index lags the QBO index by 6–7 months, and maximum positive correlations exist when the NINO3.4 index leads the QBO index by 8–10 months, which implies that El Niño events tend to peak in about half a year after the maximum easterly QBO winds at 30 hPa.

Based on the QBO time scale component of U30, HHKWK divided a full QBO life cycle into eight phases, phase 1: westerly anomaly developing period; phase 2: westerly peaking period; phase 3: westerly decaying period; phase 4: westerly to easterly transition period; phases 5 and 6: easterly anomaly developing period; phase 7: easterly anomaly peaking period; and phase 8: easterly anomaly decaying period. Following the phases of evolution within a composite QBO life cycle, HHKWK concluded that the connection of the QBO with the tropospheric anomalies is associated with the vertical propagation of the anomalies in the lower stratosphere and troposphere. While the QBO signals in the lower stratosphere propagate systematically downward, temperature anomalies develop also in the troposphere and propagate upward. Downward and upward propagating anomalies meet near the tropopause between 200 and 100 hPa one to two phases after the peak of the SSTA in the equatorial Pacific. The vertical propagation in the troposphere seems to be associated with the QBO-induced fluctuations of the tropical deep convection in the western-central Pacific. Adjustment of the Walker circulation associated with SSTA in the central and eastern Pacific also plays an active role in the connection between the SSTA and QBO (Gray et al. 1992a, b; HHKWK).

Overall, HHKWK suggested that there is some kind of interaction between the QBO and tropospheric climate variability. For example, in some phases of a QBO cycle, different zonal wind and thermal structure may affect the characteristics of the atmospheric stability and the Walker circulation as well as the evolution of SSTA along the tropical Pacific Ocean. In a sense, the connection of the QBO with tropical Pacific SST is similar to the rectification mechanism of the Madden-Julian Oscillation into the ENSO cycle (Kessler and Kleeman 2000).

Our further examination shows that the QBO-SST relationship has experienced significant interdecadal modulation during past five decades. As an extension to Part I of this work, in Part II, we examine the interdecadal variations of the connection between the QBO and tropical SST, as well as the general circulation in the troposphere, including the Walker circulation and atmospheric stability. The paper is organized as follows. The interdecadal variations of the connection between the QBO and tropical SST are described in Sect. 2. A physical explanation is given in Sect. 3. Section 4 provides conclusions and discussion.

2 Interdecadal variations of the connection between the QBO and tropical SST

HHKWK examined the lead-lag correlations between a QBO index, defined as the EEMD mode of U30 with dominant quasi-biennial period at the grid point closest to Singapore, and tropical Pacific NINO3.4 index, which suggested that on average a cold event usually follows the westerly peaking phase at 30 hPa by about 6 months. To demonstrate the interdecadal change of the relationship during the past several decades, Fig. 1a and b display the lead and lag correlations between the NINO3.4 and QBO indices with a 20-years running window for the raw data of the ERA40 and NCEP/NCAR reanalyses. It is seen that there are significant interdecadal variations in lead and lag correlations, which are similar between the two reanalyses. During 1966–1974, there are maximum positive correlations when the NINO3.4 index leads the QBO by about 11–13 months or lags by about 12–18 months. The maximum negative correlations appear when the NINO3.4 index lags the QBO index by about 0–6 months while the contemporary correlation between the QBO and NINO3.4 indices is weakly negative.

During 1975–1979, both the contemporary and lagged correlations are relatively small and the QBO and ENSO were practically unrelated to each other. A noticeable shift happened during 1978–1980 (see the vertical dashed line in Fig. 1). During 1980–1992, although the contemporary correlation between the QBO and NINO3.4 indices is small, the maximum negative correlations appear when the NINO3.4 index lags the QBO index by about 3–12 months. The positive correlations are over 0.3 when the NINO3.4 index lags the QBO index by 12–18 months. Overall, this represents a shift of the phase relation between the QBO and the tropical Pacific SST with an increased delay of the later from the former. This tendency seems to progress gradually during the 1980s, as seen by the downward tilting of the maximum correlations in Fig. 1a and b. In about 1995, there was another shift of the lead and lag

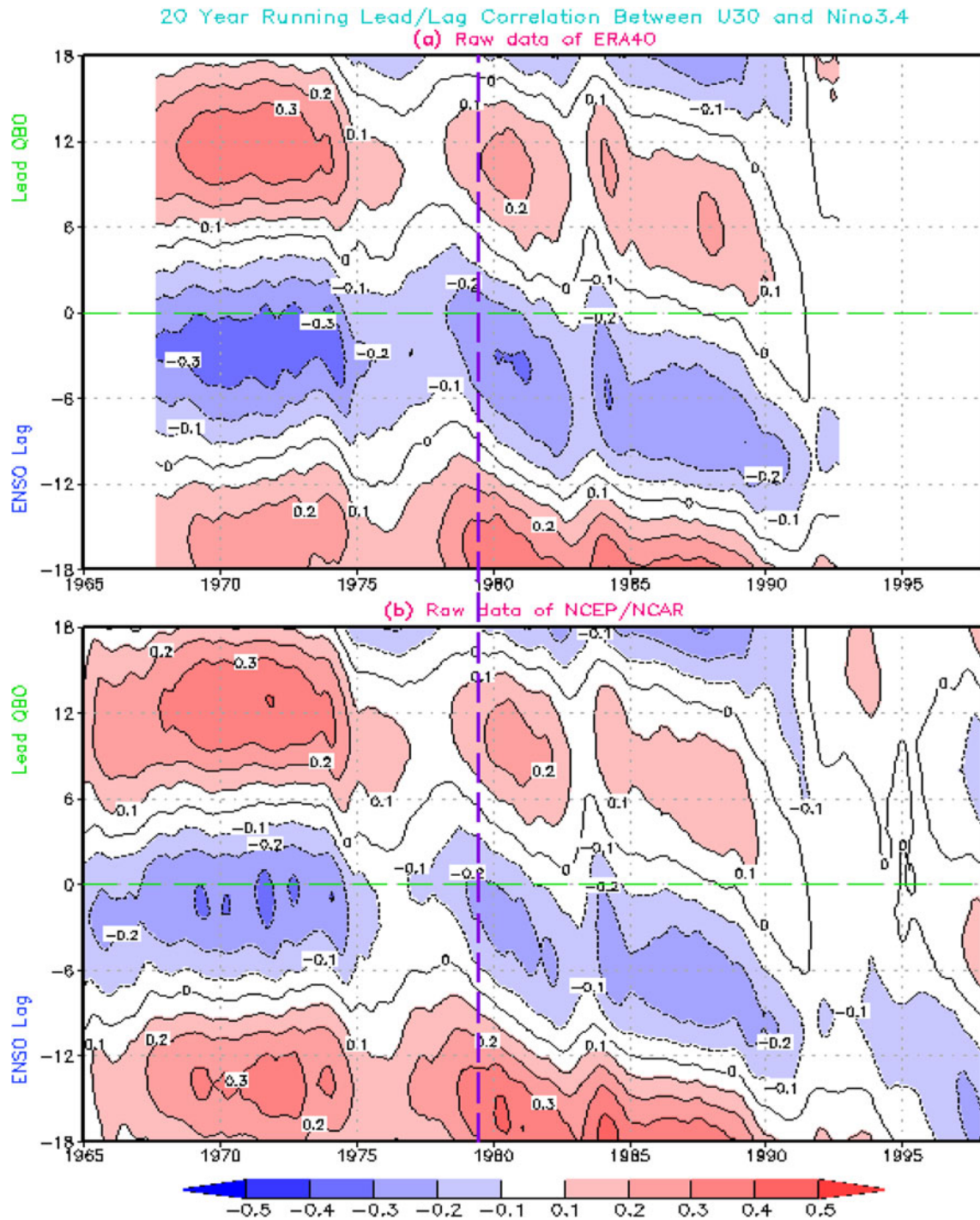


Fig. 1 Lead and lag correlations with a 20-years running window between the NINO3.4 index and U30 at the grid point closest to Singapore for raw data from the ERA40 (a), and NCEP/NCAR

reanalysis (b). Contour interval is 0.1. Positive (*negative*) values on the Y axis are the numbers of months that the NINO3.4 index leads (*lags*) U30. The vertical dashed line is for August 1979

correlations in the NCEP/NCAR reanalysis (Fig. 1b). The correlation coefficient almost reverses sign after about 1995, compared with the averaged pattern before 1975 in the NCEP/NCAR reanalysis.

Similarly, we calculate lead-lag correlations of the QBO index with the C4 and C3 + C4 components of

EEMD (Fig. 2) of the NINO3.4 index, which, respectively include 3-years and the combined 1.5-years and 3-years bands which are the dominant time scales of the ENSO variability. The interdecadal changes in the QBO correlations with these filtered indices are consistent with those derived from the raw SST data, suggesting that

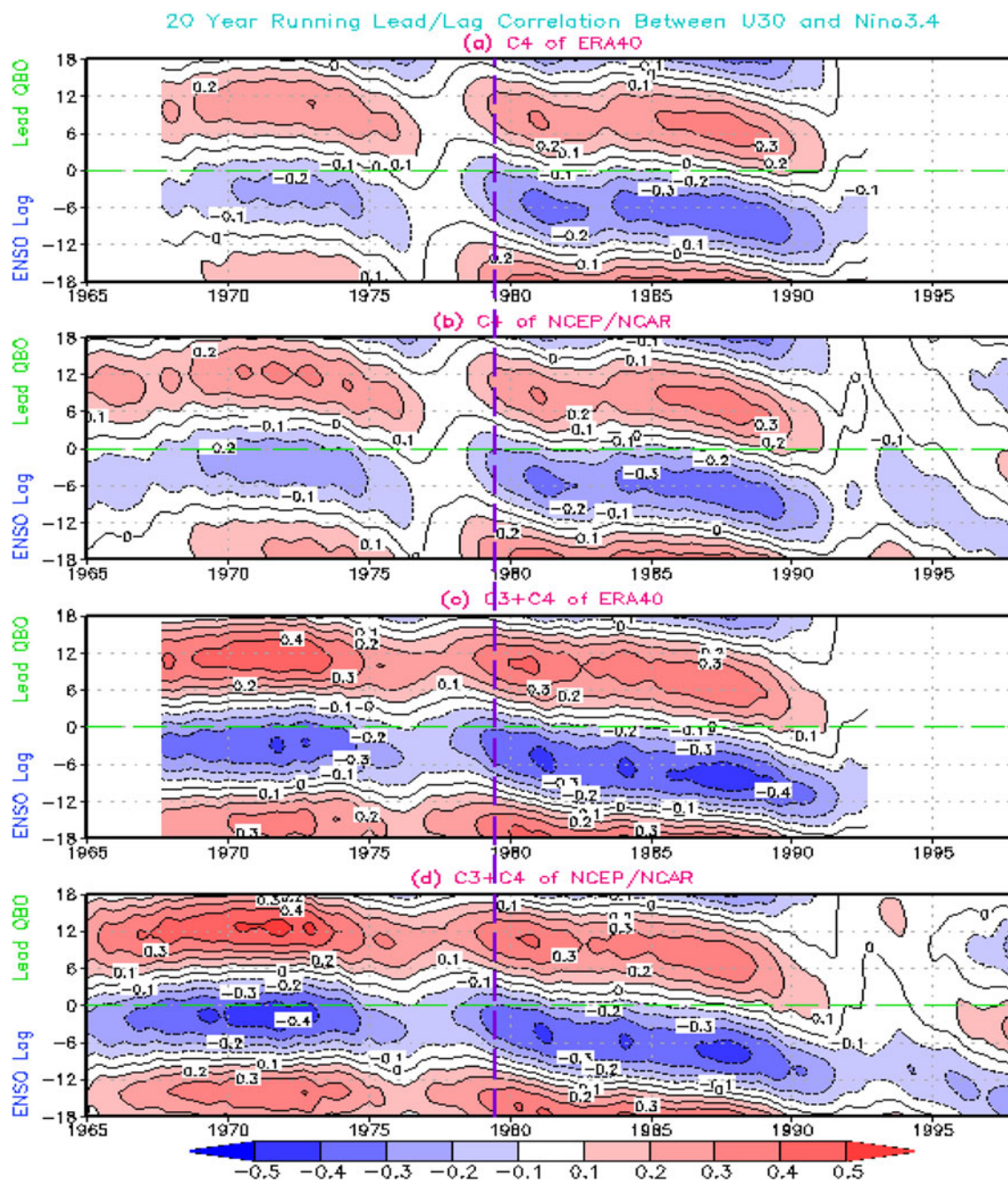


Fig. 2 Lead and lag correlations with a 20-years running window between the NINO3.4 index and U30 at the grid point closest to Singapore for the C4 component of the ERA40 (a), and NCEP/NCAR reanalysis (b), and C3 + C4 component of the ERA40 (c), and

NCEP/NCAR reanalysis (d). Contour interval is 0.1. Positive (*negative*) values on the Y axis are the numbers of months that the NINO3.4 index leads (*lags*) the U30. The vertical dashed line is for August 1979

these changes originate from the interdecadal modulation of the QBO-ENSO phase relation on these time scales. Qualitatively, the correlations are slightly improved with the combined C3 and C4 components of the NINO3.4 index than either the raw data or the C4 component alone. It seems to suggest that the multidecadal shift mainly originates from the modulation of the interannual bands of the NINO3.4.

To further confirm the interdecadal shift of the connection between the QBO and the tropical SSTA, we split the ERA40 data into two subsets, September 1957–August 1979 (referred to as earlier period) and September 1979–August 1994 (referred to as later period), and recalculate the QBO life cycle composites using each subset. The composites are computed based on the eight phases of the QBO determined by the C4 component of the EEMD of

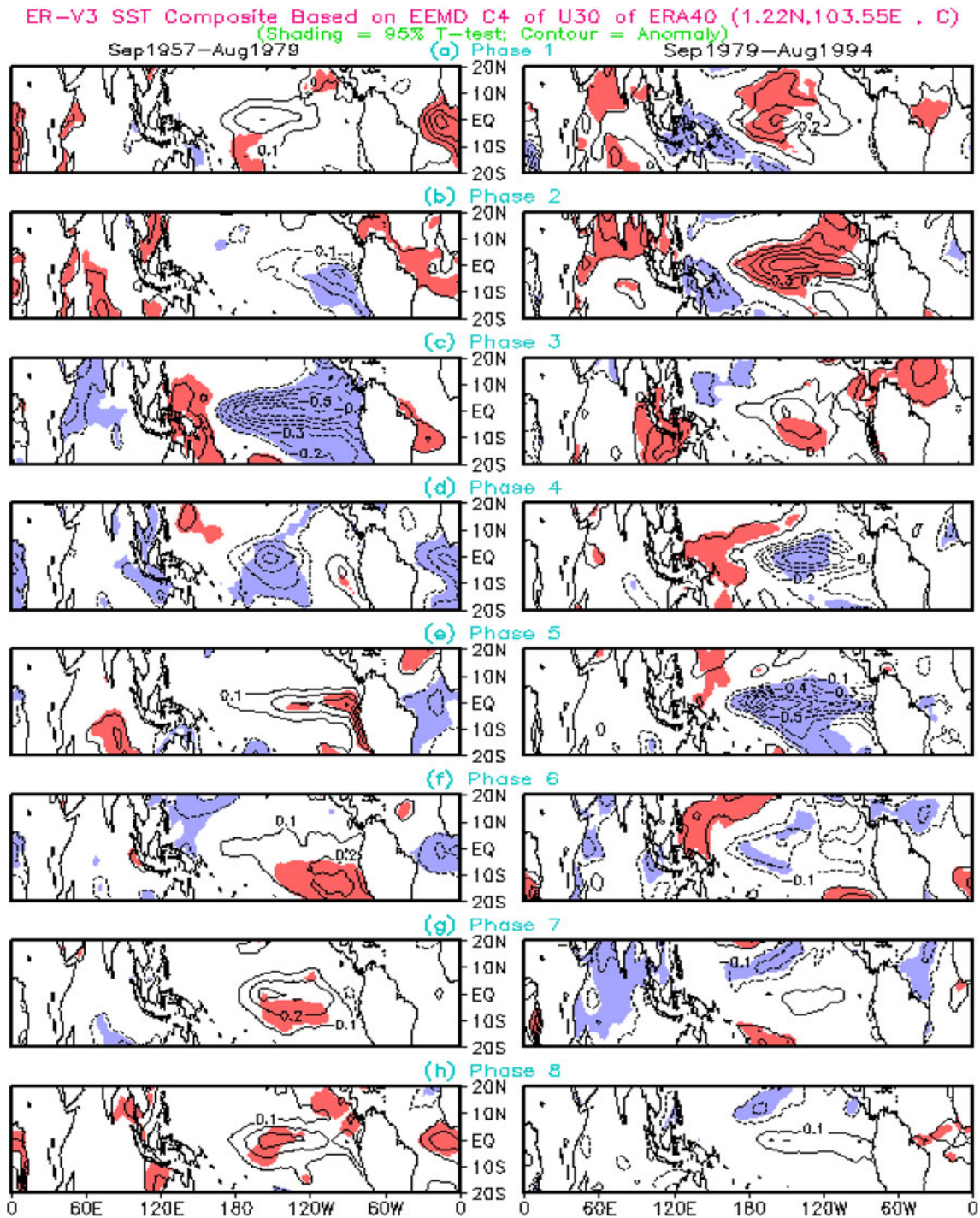


Fig. 3 QBO life cycle composites of tropical SSTA according to the phases determined by the EEMD C4 component of U30 at the grid point closest to Singapore and its tendency from the ERA40 for the

periods of Sep. 1957–Aug. 1979 (*left panel*) and Sep. 1979–Aug. 1994 (*right panel*). The shading represents 95% significance using a student's *t* test. Contour interval is 0.1°C

U30 and its time tendency in the same way as HHKWK. Our composite results are not sensitive to the exact cut-off year between these two periods. We limit our scope of analysis within these two periods because longer observations are needed to confirm the more dramatic shift after 1995 (Fig. 1).

The SST composites for both periods are displayed side by side in Fig. 3. Basically, the associated evolutions between the QBO and the tropical SSTA composites for the earlier period (*left panel* of Fig. 3) are similar to those for the whole period in HHKWK. In contrast, the composite for the later period show a different SST evolution

pattern with respect to the QBO life cycle, although the amplitudes of the SSTA are comparable for both periods (Fig. 3). For instance, in the earlier period composite (left panel of Fig. 3), cold SSTA first appear in the eastern Pacific in phase 2, which peak while extending to the dateline in phase 3 before decaying in phase 4. The warm SSTA then initiate in phases 4–5, peak in phases 7–8, and finally evolve into SST anomalies similar to that for the phase 1. It is interesting to note some asymmetry in a cycle of SST evolution: Though spanning longer time, the development of the warm phases is not as strong and well organized as that of the cold phases. For the later period composite (right panel of Fig. 3), the developments of the warm and cold phases are more similar to each other although the warm phases still span longer. The main difference of the evolution of the composite SSTA between the two periods, however, is that the sequence for the later is delayed by about two phases (about 6–7 months), with major cold anomalies occurring in phases 4 and 5 while the warm anomalies occur in phase 8 and peak in phases 1 and 2.

The evolutions of the composite SST anomalies in both periods are closely linked with the composites evolutions of the wind and geopotential height (H1000) anomalies at 1000 hPa, which characterize the variations of the sea level pressure and surface wind (Fig. 4). When cold SSTA is strong in the equatorial Pacific, the H1000 is positive (high H1000, red shadings) in the eastern and central tropical Pacific but negative (low H1000, blue shadings) to the west of 150°–160°E. There are also asymmetric behaviors in the wind and H1000 composites, corresponding to the asymmetry between the warm and cold SSTA described above. For September 1957–August 1979, strong zonal wind anomalies and east–west H1000 gradient are prominent in the cold SSTA, but it is much less clear in the warm SSTA (left panel of Fig. 4). However, the situation is nearly opposite for September 1979–August 1994 (right panel of Fig. 4).

These interdecadal variations of the association between the QBO and tropical Pacific SSTA may be a contributing factor in the differing conclusions about possible QBO–ENSO relationship in the previous investigations. For example, through analyzing different datasets for different periods, some studies (e.g., Maruyama and Tsuneoka 1988; Yasunari 1989; Angell 1992) suggested the existence of their co-variability, while others (e.g., Quiroz 1983; Barnett 1991; Xu 1992) did not find solid evidence for the existence of such a connection. Furthermore, Taguchi (2010) suggested that ENSO may affect the QBO though modulating wave flux: the QBO signals exhibit weaker amplitude and faster phase propagation for El Niño conditions. These controversies might also be caused by the differences in the definitions of the QBO in these studies,

for example, to measure the QBO, zonal wind at 50 hPa was used in Holton and Tan (1980), averaged zonal wind anomalies in 70–10 hPa in Gray et al. (1992a), first two leading Empirical Orthogonal Function (EOF) modes of zonal wind anomalies in layers 70, 50, 30, 20, 15, and 10 hPa in Wallace et al. (1993), extended EOF in Wang et al. (1995), zonal wind difference between two layers in Huesmann and Hitchman (2001), and trajectories in a phase space spanned by time series of two leading EOF modes of wind variability in Taguchi (2010).

3 Possible physical causes for the interdecadal shifts in the QBO–ENSO relationship

From the above discussion, we saw a clear interdecadal variation of the connection between the QBO and tropical Pacific surface climate variability (including SST, wind and geopotential height at 1,000 hPa). To interpret the interdecadal variation, it is necessary to check the consistency of the whole troposphere and lower stratosphere along the equatorial Pacific with the interdecadal variations of the connection. Similar to the composites of SSTA in Fig. 3, we first compute and examine the QBO life cycle composites of various variables (zonal wind, temperature, Walker circulation, equivalent potential temperature θ_e) anomalies between the surface and 10 or 50 hPa averaged between 5°S and 5°N for the two different periods according to the phases determined by the EEMD C4 component of U30 and its tendency. Then, we investigate the contribution of the characteristic change of the ENSO and irregularity of the QBO to the interdecadal change of the relationship between the QBO and the troposphere climate in the tropical Pacific.

3.1 Decadal variation of the QBO associated vertical circulation

Figures 5 and 6 show the QBO life cycle composites of zonal wind anomalies between the surface and 10 hPa averaged between 5°S and 5°N according to the phases determined by the EEMD C4 component of U30 and its tendency for the earlier and later periods, respectively. In each figure the left panel presents the composite from the ERA40 while the right one is for the NCEP/NCAR reanalysis. Both reanalyses show broadly consistent features. In the stratosphere, both Figs. 5 and 6 display analogous patterns associated with the QBO, which are consistent with HHKWK. However, there are some quantitative differences in the phase composites between the earlier and later periods in the troposphere below 100 hPa, which may be of significance for the analysis here. For example, in the earlier period composite (Fig. 5), there is a

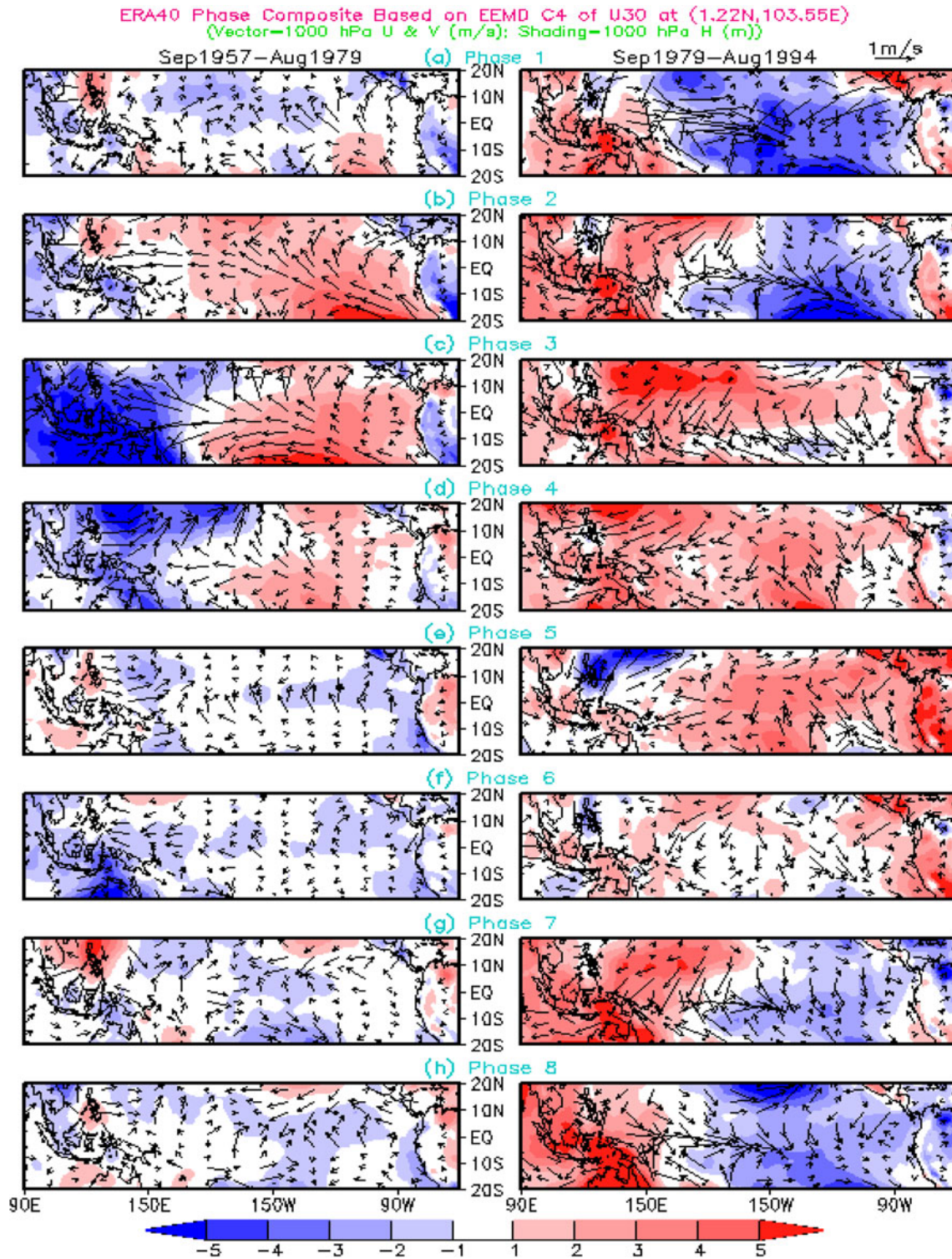


Fig. 4 QBO life cycle composites of geopotential height (shading) and surface wind (vector) anomalies at 1,000 hPa of ERA40 over the tropical Pacific Ocean. The phases are determined by the EEMD C4 component of U30 from the ERA40 at the grid point closest to

strong downward penetration of the westerly wind anomalies near the dateline in phase 3 (Fig. 5c) and, to a lesser extent, a similar downward penetration of the easterly wind

Singapore and its tendency. The composites are made separately for the periods of Sep. 1957–Aug. 1979 (left panel) and Sep. 1979–Aug. 1994 (right panel)

anomalies occurs in phase 7 (Fig. 5g). In the earlier period, these fast propagating, nearly barotropic wind anomalies are confined to the regions near the dateline, which implies

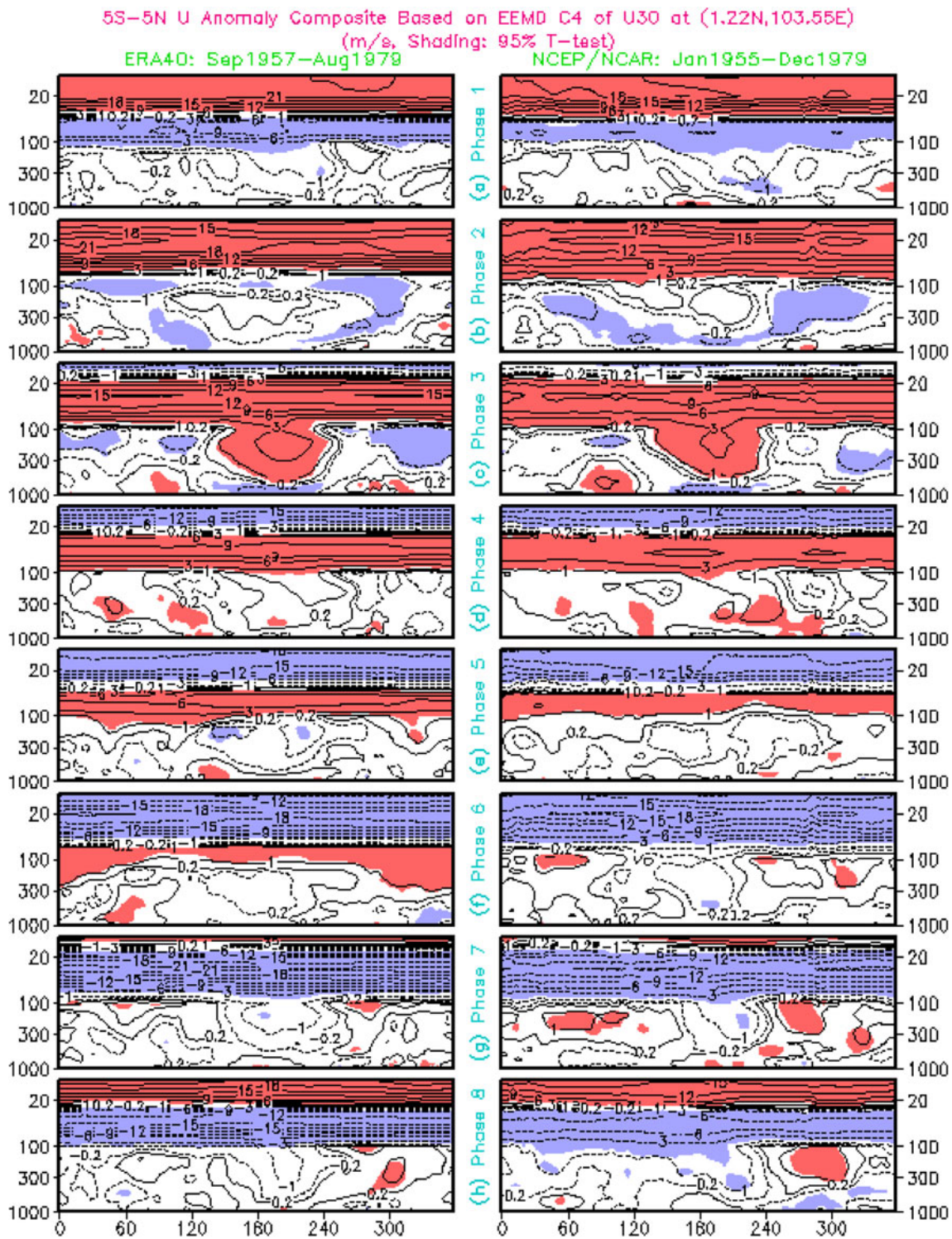


Fig. 5 QBO life cycle composites of zonal wind anomalies along the equator between the surface and 10 hPa averaged between 5°S and 5°N according to the phase determined by the EEMD C4 component of U30 at the grid point closest to Singapore and its tendency from the ERA40 in

Sep. 1957–Aug. 1979 (left panel) and from the NCEP/NCAR reanalysis in Jan. 1955–Dec. 1979 (right panel). The shading represents 95% significance using the student's *t* test. Contours are $-21, -18, -15, -12, -9, -6, -3, -1, -0.2, 0.2, 1, 3, 6, 9, 12, 15, 18,$ and 21 with unit of m/s

that this is a sensitive region for troposphere-stratosphere interaction. Moreover, the fast downward propagation of the QBO wind anomalies from the stratosphere into the

troposphere may affect the wind anomalies within the troposphere. Since the composite represents an average of many events, it may make the transition smoother than in

individual events, which could be more abrupt in some extreme cases. Nevertheless, the phase composite procedure may better preserve its general characteristics of propagation than other alternatives, e.g., averaging based on calendar months. Although we cannot rule it out, this feature is unlikely dominated by one or two extremely strong event, given its quite large magnitude in the composites (Fig. 5c). More detailed case study should be conducted to understand the nature of this process, which is beyond the scope of this paper.

Before the downward extension of the westerly wind anomalies in phase 3, easterly wind anomalies seem to prevail from phase 8 (Fig. 5h) to phases 1 and 2 (Fig. 5a, b) within the troposphere, although other features of the tropospheric circulation obscure this signal. The easterlies are consistent with the downward propagating QBO signals from the lower stratosphere. The downward westerly wind anomalies in phase 3 interrupt the tropospheric easterlies and set up a period of westerly anomalies in the troposphere in phases 4–5. Although on average, the QBO is a zonally uniform phenomenon in the stratosphere, this uniformity breaks down near the tropopause during these phases. The composites for the later period (Fig. 6), however, show a different picture in the troposphere. In this period, there is no apparent abrupt downward propagation near the dateline as shown in phase 3 of the earlier period (Fig. 5). Instead, although obscured by noise, the QBO signals propagate more slowly in the troposphere and arrive at the lower troposphere about two phases later than in the earlier period (Fig. 6e). These differences also show up in a consistent way in Walker circulation composite.

The QBO life cycle composites of the anomalous Walker circulation according to the QBO phases are shown in the left panel of Fig. 7 for the earlier period and right panel of Fig. 7 for the later period in the ERA40. There are some significant differences between the two period composites. For example, a noticeable subsidence occurs first in the western equatorial Pacific in phase 2 for the earlier period (left panel of Fig. 7b), which then grows rapidly and shifts eastward in the next two phases. Interestingly, the major subsidence in phases 3–4 near and to the east of the dateline (left panel of Fig. 7c, d) was observed, while the downward wind propagation occurs in phase 3 (Fig. 5c). This strong subsidence in the central Pacific, together with the increased ascending motion to its west, seems to imply a westward shift of the convective center in the western Pacific. This speculation is consistent with the zonal H1000 gradient and surface wind anomalies over the equator in these two phases (left panel of Fig. 4c, d). The subsidence in the central Pacific is quickly replaced by weak ascent motion in phase 5 (left panel of Fig. 7e), which persists and shifts eastward in the next several phases (left panel of Fig. 7f–h), as well as phase 1 (left panel of Fig. 7a). Warm

Pacific SSTA accompanies these ascent phases in the central and eastern Pacific (left panel of Fig. 3). For the later period, although a significant subsidence also occurs in phase 2 over the western Pacific (right panel of Fig. 7b), its growth and eastward shift are slower, which spans from phase 3 to phase 6 (right panel of Fig. 7c–f). They roughly coincide with the development of a cold episode in the tropical Pacific (right panel of Fig. 3d–f).

The Walker circulation anomalies are in line with the temperature anomalies (Fig. 8). There are robust anomalies and differences between the two period composites in both the troposphere and lower stratosphere (Fig. 8). The structures of temperature anomalies above 100 hPa are similar between the two composites in almost all phases (Fig. 8), which represent the downward propagating QBO signal. Similar to the SST and zonal wind composites (Figs. 3, 4, 5, and 6), there is also a two-phase delay in the upward propagation of temperature anomalies from lower to upper troposphere between the earlier and later periods (Fig. 8). For example, the maximum descending motion and troposphere cooling occur in phase 3–4 for the earlier period (left panel of Figs. 7c, d and 8c, d) and in phase 5 for the later period (right panel of Figs. 7e and 8e).

To further demonstrate the contrast of the stratification in the two periods, Fig. 9 shows the phase dependence of the vertical temperature anomalies in the ERA40 averaged in 5°S–5°N, 150°–120°W in the earlier and later periods. The results in Fig. 9 are consistent with that in Figs. 7 and 8. In the earlier period (Fig. 9a), the negative (positive) temperature anomalies propagate downward from the lower stratosphere and upward from the troposphere, and meet at the tropopause. That is in line with HHKWK for the whole data period. On average, the anomalies have opposite signs between the troposphere and lower stratosphere, which favor to alter the vertical stratification around the tropopause. For example, in phases 3–4, cooling in the troposphere and warming in the lower stratosphere are apparent, which may be connected with the quick development of the subsidence anomalies (left panel of Figs. 7a–d, 9a).

In contrast to the earlier period, the later period (Fig. 9b) shows some different features. The opposite sign anomalies between the troposphere and lower stratosphere are less visible. For example, it is almost in phase for the anomalies in the troposphere and lower stratosphere in phases 2–3 (Fig. 9b). Similarly, the temperature anomalies appear after a delay of about two phases in the later period composite than in the earlier period composite. For example, the negative anomalies in the troposphere exist in phases 2–4 for the earlier period, in phases 4–6 for the later period. A similar shift occurs for the positive anomalies. The anomalies for the corresponding composite using the NCEP/NCAR reanalysis (not shown) display features

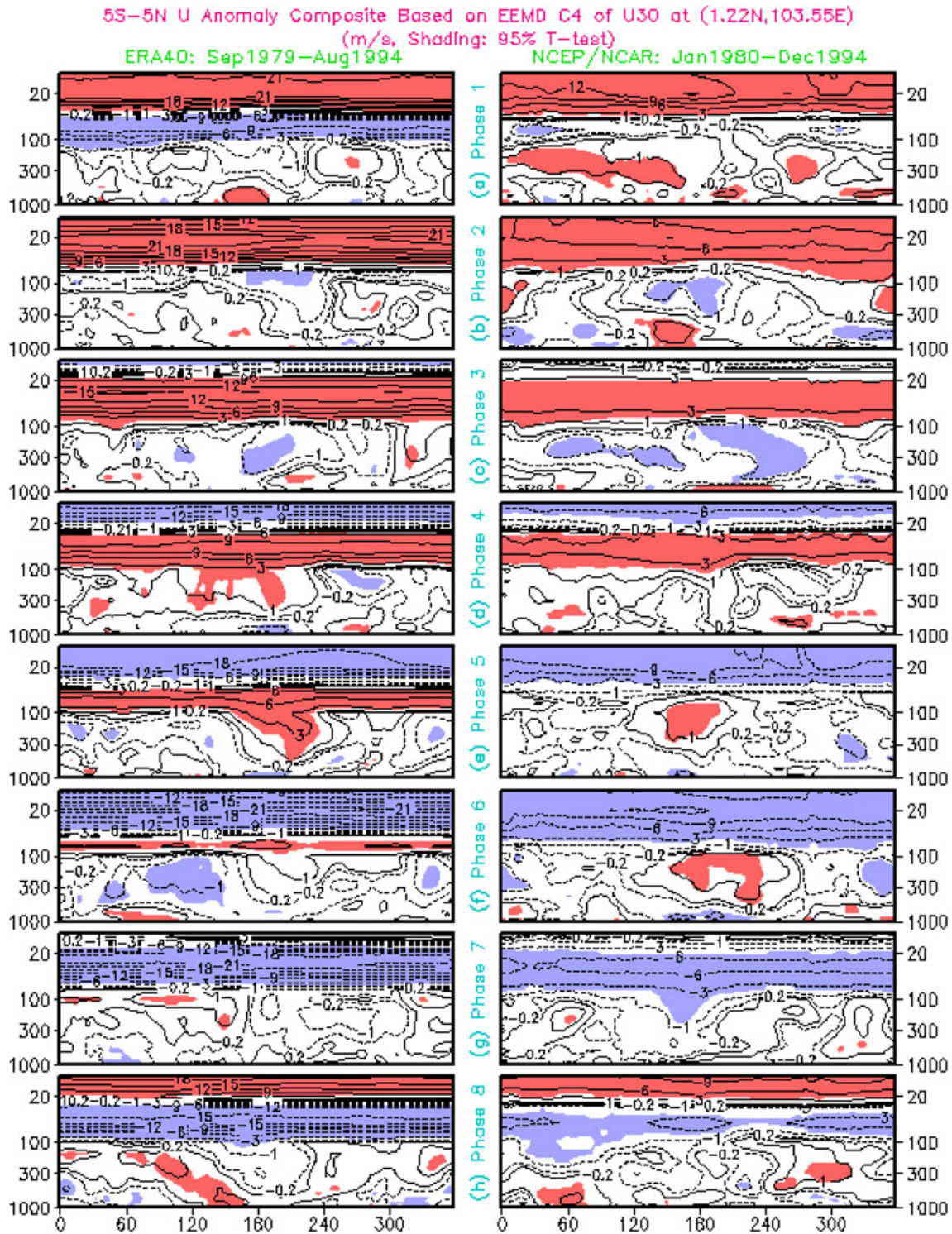


Fig. 6 QBO life cycle composites of zonal wind anomalies along the equator between the surface and 10 hPa averaged in 5°S–5°N according to the phase determined by the EEMD C4 component of U30 at the grid point closest to Singapore and its tendency from the ERA40 in Sep. 1979–

Aug. 1994 (left panel) and from the NCEP/NCAR reanalysis in Jan. 1980–Dec. 1994 (right panel). The shading represents 95% significance using the student's *t* test. Contours are $-21, -18, -15, -12, -9, -6, -3, -1, -0.2, 0.2, 1, 3, 6, 9, 12, 15, 18,$ and 21 with unit of m/s

similar to that of the ERA40, although the anomalies in the later period composite of the NCEP/NCAR reanalysis are less regular and much weaker.

These results suggest that the contrast of the temperature anomalies between the troposphere and lower stratosphere in different phases of QBO alter the vertical stratification

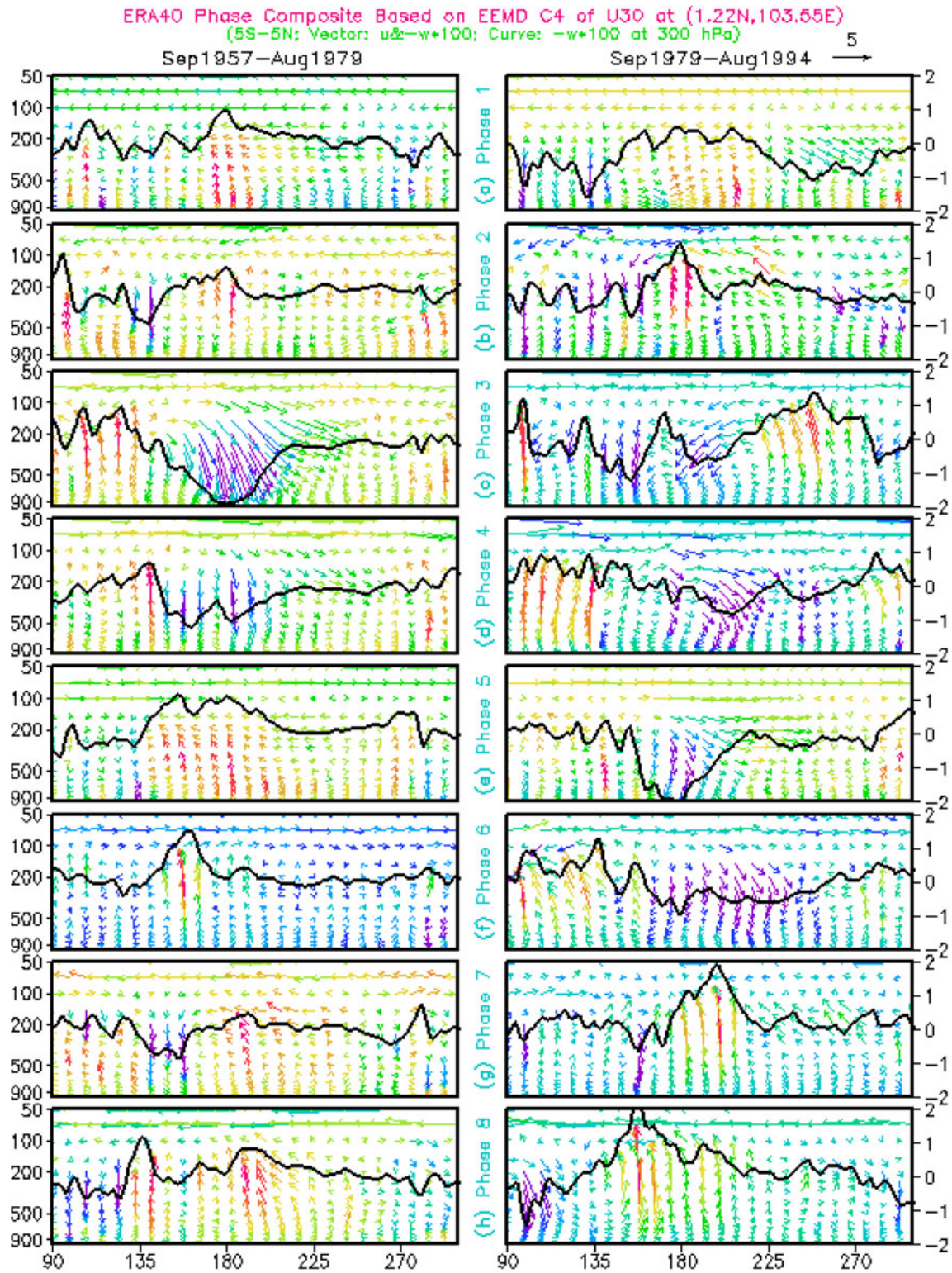


Fig. 7 Longitude-height section of QBO life cycle composites of zonal and vertical winds (vectors), and vertical velocity at 300 hPa (solid line) averaged between 5°S and 5°N in phases 1–8 according to the phases determined by the EEMD C4 component of U30 at the grid

point closest to Singapore and its tendency from the ERA40 in Sep. 1957–Aug. 1979 (left panel) and Sep. 1979–Aug. 1994 (right panel). The vertical velocity is defined as $-100 \cdot \omega$, where, ω is the vertical velocity in pressure coordinates

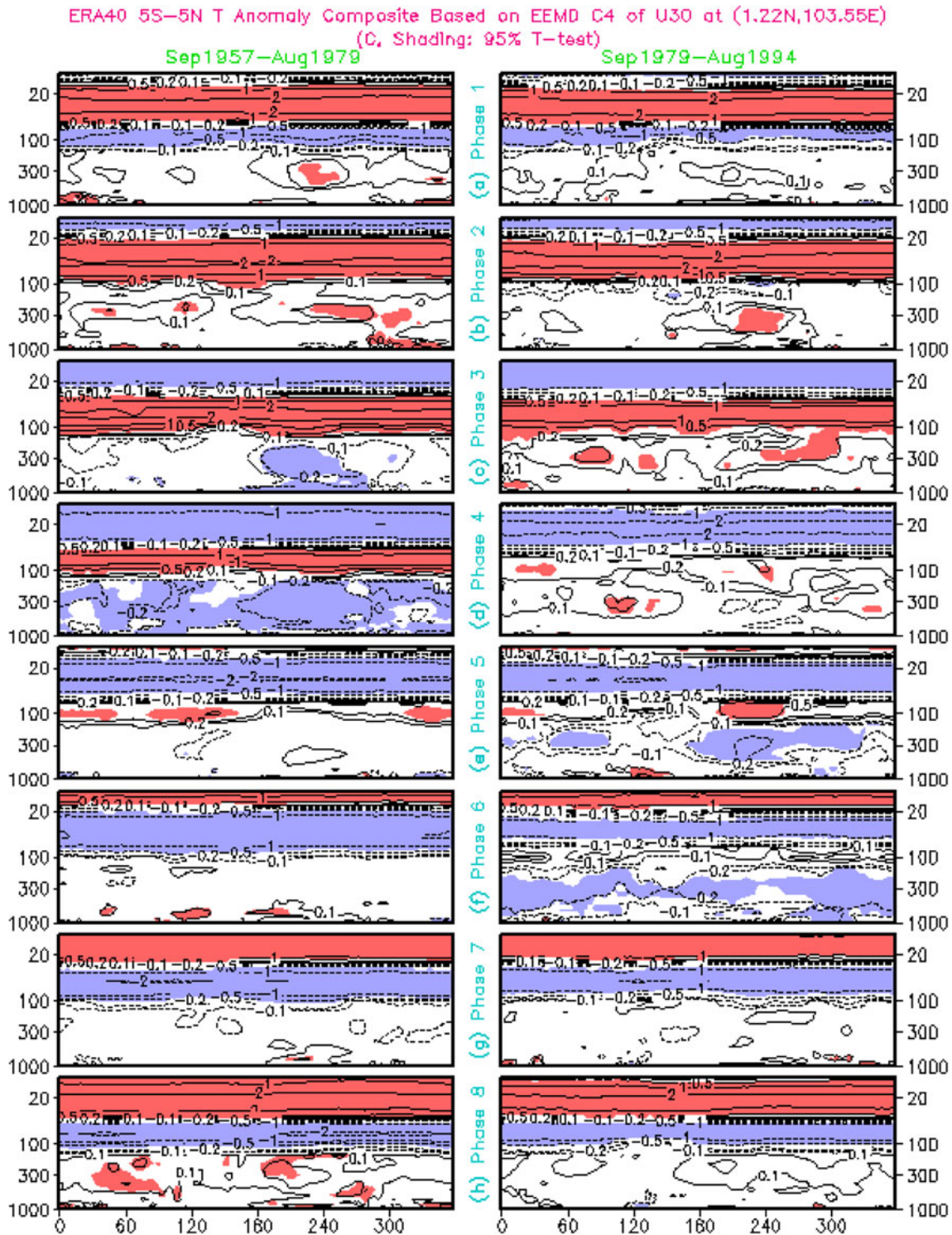


Fig. 8 QBO life cycle composites of temperature anomalies along the equator between the surface and 10 hPa averaged in 5°S–5°N according to the phase determined by the EEMD C4 component of U30 at the grid point closest to Singapore and its tendency from the

ERA40 in Sep. 1957–Aug. 1979 (left panel) and in Sep. 1979–Aug. 1994 (right panel). The shading represents 95% significance using the student's *t* test. Contours are $-4.0, 2.0, -1.0, -0.5, -0.2, -0.1, 0.1, 0.2, 0.5, 1.5, 2.0, 4.0$ with unit of °C

around the tropopause (Gettelman and Forster 2002), and may promote or suppress the deep convection in the troposphere during certain QBO phases. This contrast,

however, is not determined by the QBO evolution alone. It also involves the current state of the tropospheric temperature. Thus, we speculate that different vertical temperature

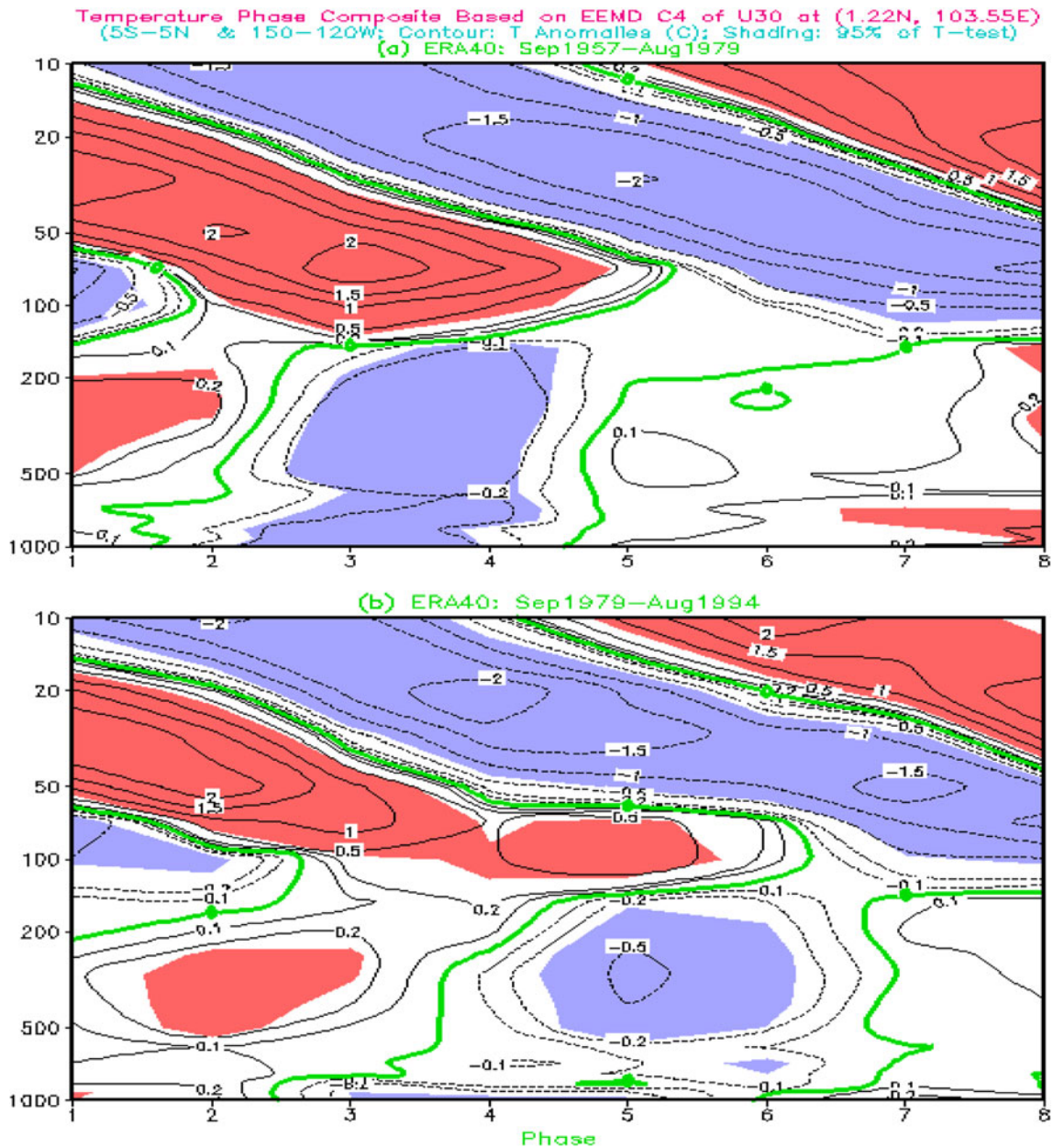


Fig. 9 QBO life cycle composites of temperature anomalies along the equator between the surface and 10 hPa averaged in the tropical eastern Pacific (5°S–5°N, 150–120°W) according to the phases determined by the EEMD C4 component of U30 and its tendency for

the ERA40 in Sep. 1957–Aug. 1979 (a), and Sep. 1979–Aug. 1994 (b). The shading represents 95% significance of the composite using the student's *t* test. Contours are –2, –1.5, –1.0, –0.5, –0.2, –0.1, 0.0, 0.1, 0.2, 0.5, 1.0, 1.5, and 2.0 with the unit of °C

stratifications may determine the different patterns of deep convection varied with the QBO phases in these two periods, which is demonstrated in the θ_e anomaly composite in Fig. 10. For instance, in the earlier period, following the enhancement of the warming in lower stratosphere and the cooling in the troposphere from phase 2 to 4 (left panel of Fig. 8b–d), the troposphere becomes more stable (θ_e increases with altitude) (left panel of Fig. 10b–d), and strong subsidence occurs (left panel of Fig. 7c, d). For the later period, the subsidence is weaker in

the same QBO phases possibly because the mid-troposphere is still quite warm and makes the stability weaker near the tropopause (right panel of Figs. 7b–d, 8b–d, 10b–d). For the later period, the tropospheric temperature stratification and stability conditions similar to that in phases 2–4 of the earlier period occur in phases 4–6 (right panel of Figs. 7d–f, 8d–f, 10d–f), consistent with the two phase delay of the connection between QBO and tropical Pacific SSTA in the later period compared with that in the earlier period. In phases 5–8 of the earlier period, warming (cooling) presents in the troposphere

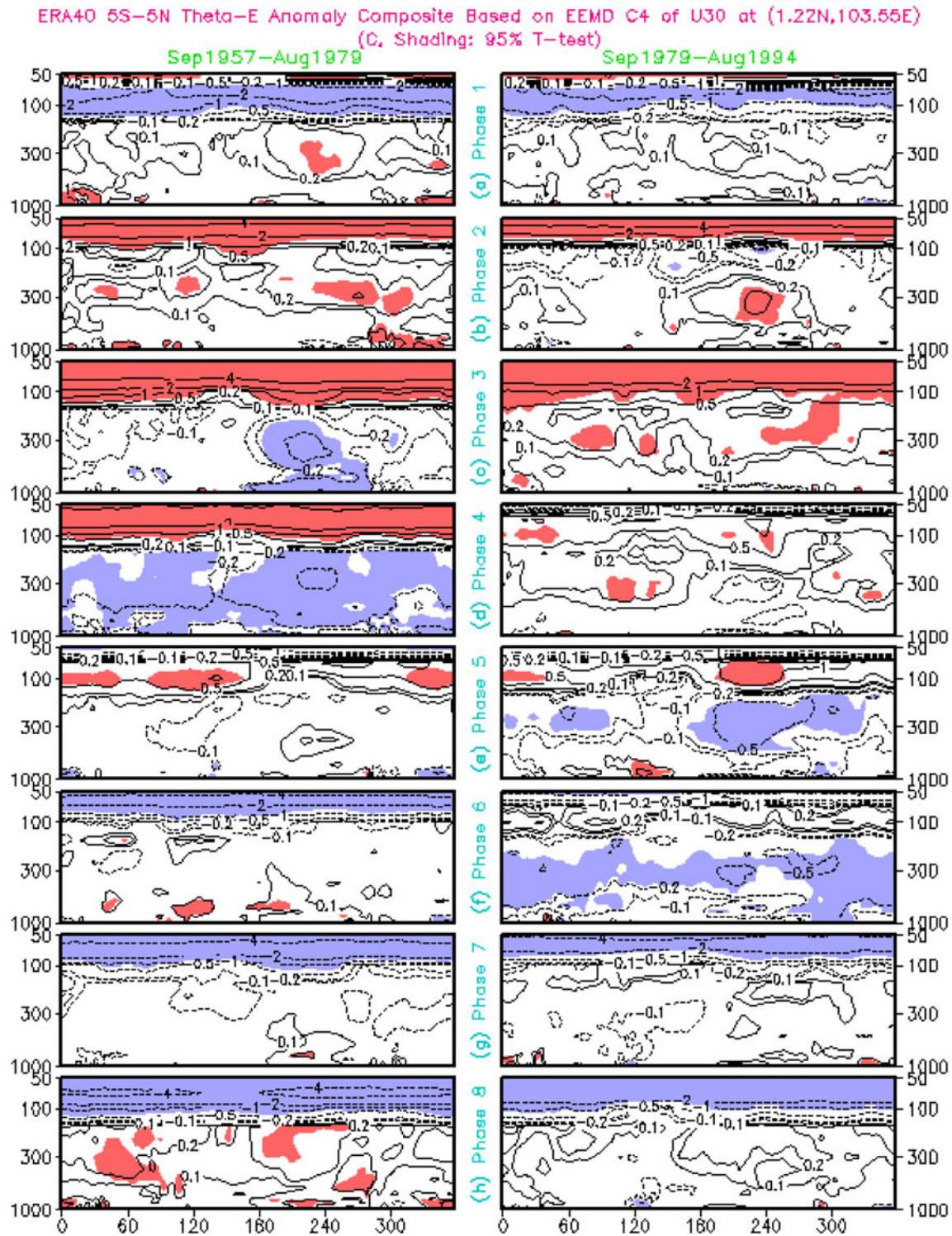


Fig. 10 QBO life cycle composites of θ_e anomalies along the equator between the surface and 50 hPa averaged in the tropical eastern Pacific (5°S–5°N, 150–120°W) according to the phases determined by the EEMD C4 component of U30 and its tendency for the ERA40 in

Sep. 1957–Aug. 1979 (left panel) and Sep. 1979–Aug. 1994 (right panel). The shading represents 95% significance of the composite using the student's *t* test. Contours are $-4.0, 2.0, -1.0, -0.5, -0.2, -0.1, 0.1, 0.2, 0.5, 1.5, 2.0, 4.0$ with the unit of °K

(lower stratosphere) (left panel of Fig. 8e–h), as a result, the troposphere becomes unstable (θ_e decreases with altitude) (left panel of Fig. 10e–h), and anomalous ascent occurs (left

panel of Fig. 7e–h). Similar situations are seen in phases 7–8, 1–2 of the later period (right panel of Figs. 7g, h, a, b, 8g, h, a, b, 10g, h, a, b).

Current results suggest that the QBO effect on atmospheric stability is dependent upon temperature anomalies in both the lower stratosphere and middle and upper troposphere that relies on both the QBO phases and ENSO phases. The physical impact of the QBO on ENSO may be largest when they match each other. Statistically, development of ascending (descending) motion seems associated with a warming (cooling) tendency in the troposphere and cooling (warming) tendency near the tropopause. The stability variation may modulate the tropical SST via altering the Walker circulation and tropical deep convections.

3.2 The contribution of the characteristic change of the ENSO

It is obvious that change in either part in the interaction loop between the QBO and the troposphere climate may result in the relationship change between them. The characteristics of ENSO have experienced notable changes since the late 1970s, which are mainly caused by a concurrent change in the background state on which El Niño evolves (Wang 1995). As an example of the different characters of the ENSO cycles in the earlier and later periods, Fig. 11 shows the lag correlations between the NINO3.4 index and global tropical SSTA for two different periods. There are some interesting changes in the characteristics of the SSTA pattern associated with the ENSO. For instance, the meridional scale is wider for the positive correlations and is narrower for the negative correlations during January 1951–December 1979 than during January 1980–December 1994. For the evolution of the negative correlations, the negative anomaly is initiated near the southern American coast in the earlier period (left panel of Fig. 11e), and near the central tropical North Pacific in the later period (right panel of Fig. 11e). For the time scale of ENSO variability, it is found that the positive correlations in the tropical eastern Pacific persist for a shorter duration in the earlier period than in the later period (compare the left and right panels of Fig. 11a–e). In addition, the amplitudes of the correlations near the dateline are larger for the positive ones and smaller for the negative ones in the earlier than in the later periods. Furthermore, the connections between the ENSO and SSTA in the tropical Atlantic and Indian Oceans also experienced some interdecadal variations. These changes are in conjunction with the changes of ENSO features, such as the onset, frequency, and the structure of the coupled ENSO mode (Wang 1995; An and Wang 2000). For example, An and Wang (2000) pointed out that oscillation period of ENSO increased from 2 to 4 years (high frequency) during 1962–1975 to 4–6 years (low frequency) during 1980–1993.

We speculate that the interdecadal change of the QBO and tropospheric circulation may therefore, be partially due to the interdecadal change in the characteristics of the ENSO. To test this hypothesis, we first construct a QBO time series with an invariant period by using a sine function with a period of 28.7 months (line in Fig. 12a). The period is determined by the power spectrum analysis in HHKWK. Then, the lead and lag correlations with a 20-years running window between the observed raw NINO3.4 index (shading in Fig. 12a) and the constructed QBO time series (line in Fig. 12a) are computed in a similar way to Figs. 1 and 2. It is found that the pattern of the correlation is similar between Figs. 1 and 12b, particularly for the long-term change of the correlation pattern. Because of regularity of the constructed QBO time series, the interdecadal variation in Fig. 12b is purely due to the change of the NINO3.4 index. Thus, the similarity between Figs. 1 and 12b suggests that the interdecadal variation of the correlation between the QBO and the tropospheric climate is largely due to the characteristic change of the ENSO. However, the quantitative differences between Figs. 1 and 12b seem to suggest the contribution of the irregularity of the QBO.

To qualitatively examine the contribution from the irregularity of the QBO to the interdecadal variation of the correlation between the QBO and ENSO, we compute the lead and lag correlation with a 20-years running window between the analyzed QBO index of ERA40 (U30 at the grid point closest to Singapore) and a constructed NINO3.4 index. Contrasting to the sharp peak of the spectrum of the QBO at 28.7 months in HHKWK, there are two relatively flat peaks of the spectrum of the ENSO indices at 2–7 years. Based on this feature of the ENSO spectrum, we use the sum of two sine functions to simulate the regularity component of the NINO3.4 index. As a first order approximation and to be simplified, we assume that the two sine functions have same amplitude with periods of 17.8 and 37.2 months, respectively. The periods are determined based on the periods of two dominant (C3 and C4) components of the EEMD results of NINO3.4 index shown in HHKWK. The analyzed QBO index (shading) and constructed NINO3.4 index (line) are displayed in 11c and the corresponding lead and lag correlations are shown in Fig. 12d. Although the correlation pattern in Fig. 12d bears some similarities with the corresponding one shown in Figs. 1 and 2, its amplitude is smaller in Fig. 12 than in Figs. 1 and 2, suggesting that the irregularity of the QBO may play a secondary role in the interdecadal variation of the relation between the QBO and tropospheric climate.

From the above analysis, it is shown that there are clearly interdecadal variations in the association between the QBO and tropical SSTA and the Walker circulation, which are mainly due to the characteristic change of the

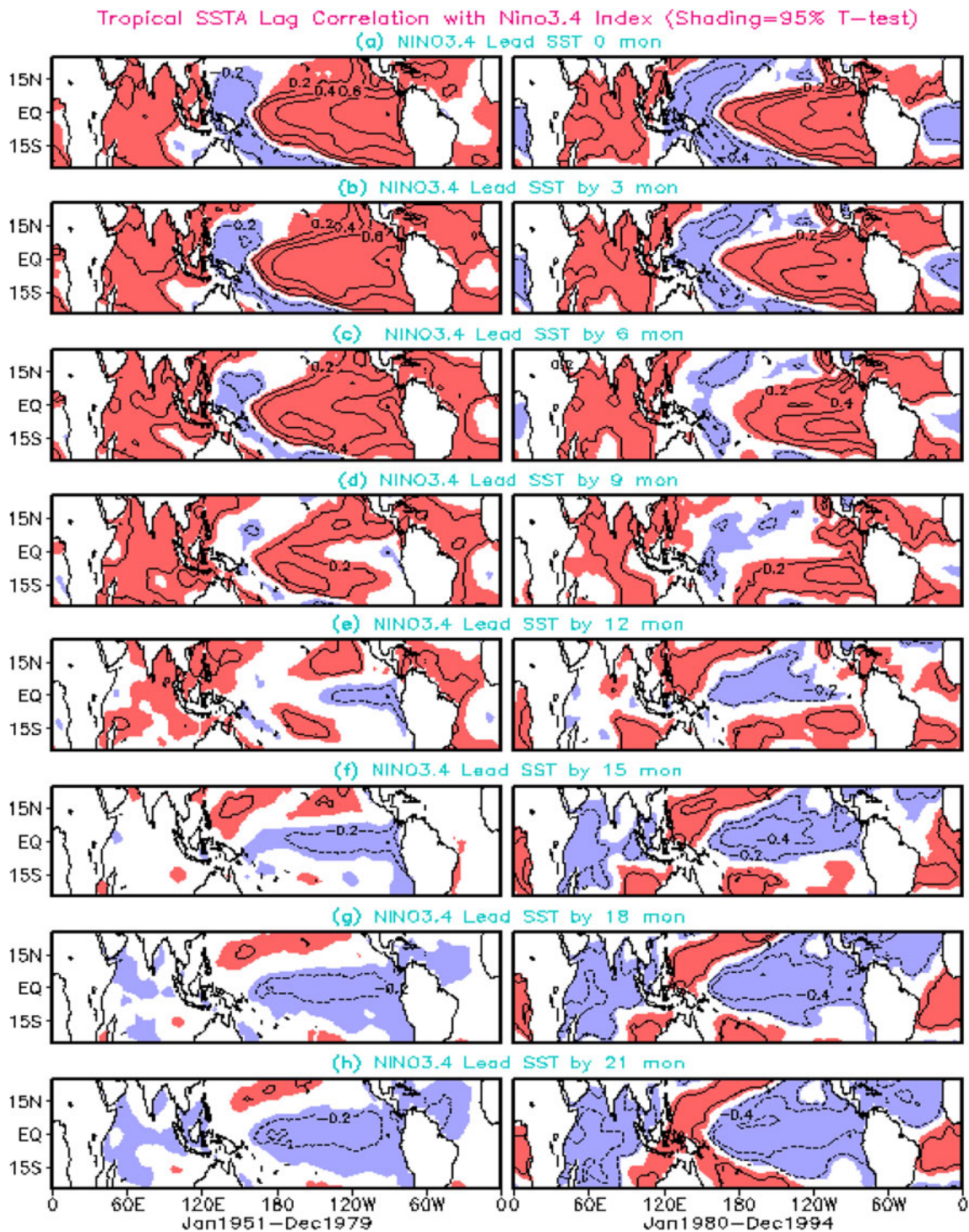


Fig. 11 Lag correlation between tropical SST and NINO3.4 index for the index leading the SST by 0 month (a), 3 months (b), 6 months (c), 9 months (d), 12 months (e), 15 months (f), 18 months (g), and

21 months (h). The *left panel* is for the period Jan. 1951–Dec. 1979, and the *right panel* is for the period Jan. 1980–Dec. 1994. The *shading* represents 95% significance. Contour interval is 0.2

ENSO. One of the characteristic changes of the ENSO is its period change, which may be a major reason causing the interdecadal variation of the association between the QBO and tropospheric climate. The interdecadal changes in the characteristics of the ENSO may be linked to the global

scale fluctuations of the climate system and the increase of the greenhouse gas concentrations. For example, the interdecadal shift of the climate system in the late 1970s is a well-documented phenomenon (Nitta and Yamada 1989; Trenberth and Hurrell 1994). On the other hand, some

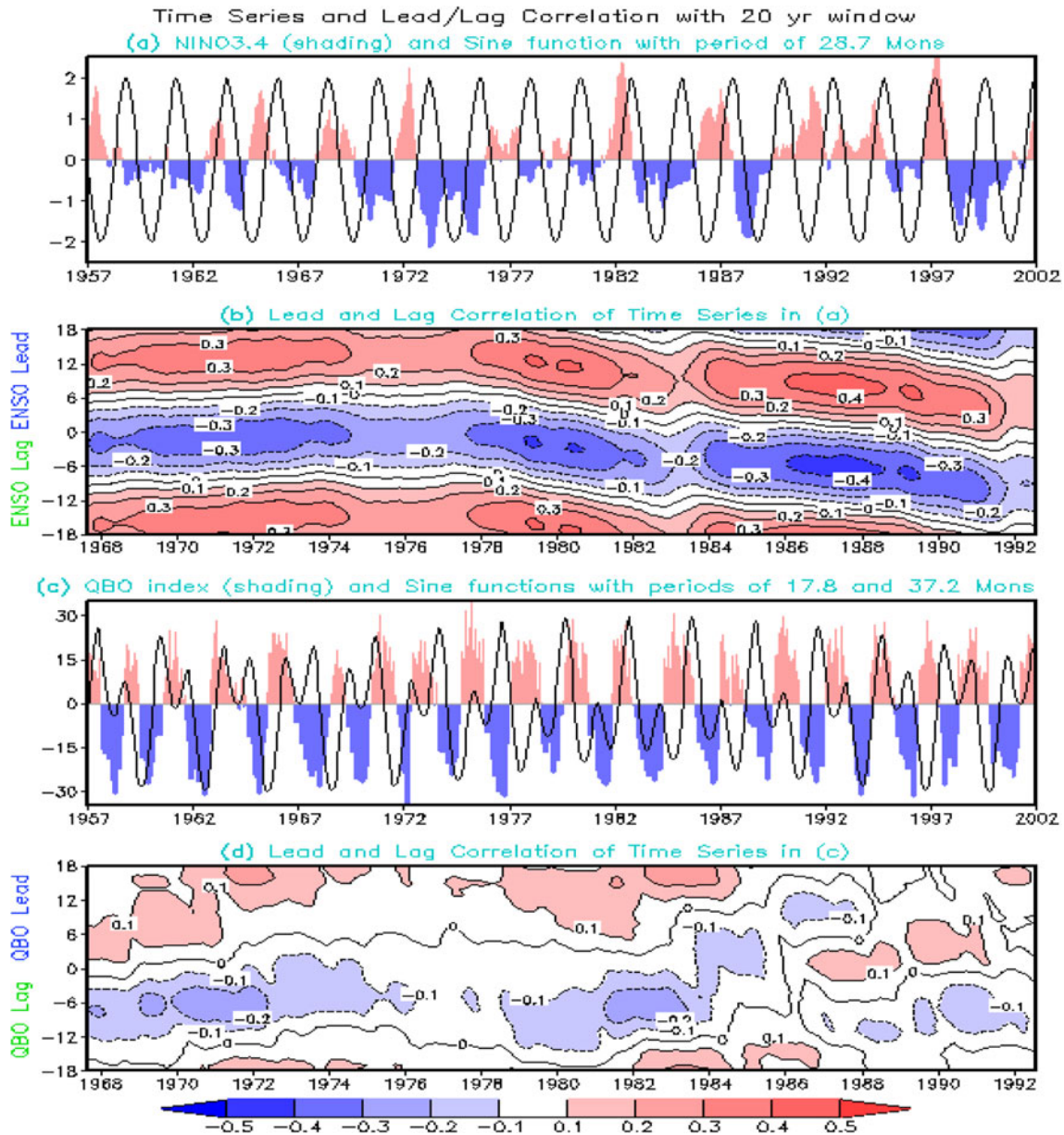


Fig. 12 **a** Time series of Nino3.4 index (shading) and sine function with period of 28.7 months (line) during Sep. 1957–Aug. 2002. **b** Lead and lag correlation with a 20-years running window between the two time series in (a). **c** U30 at the grid point closest to Singapore from the ERA40 in Sep. 1957–Aug. 2002 (shading) and the sum of

two sine functions with periods of 17.8 and 37.2 months (line) during Sep. 1957–Aug. 2002. **d** Lead and lag correlation with a 20-years running window between the two time series in (c). Contour interval is 0.1 in (b) and (d). See the text for details

model experiments suggested characteristic changes of the ENSO in future global warming scenarios (Meehl and Washington 1996; Timmermann et al. 1999; Jin et al. 2001).

4 Conclusion and discussion

The interdecadal variation of the association of the stratospheric quasi-biennial oscillation (QBO) with tropical

sea surface temperature (SST) anomalies (SSTA) and the general circulation in the troposphere and lower stratosphere has been examined using the ERA40 and NCEP/NCAR reanalyses, as well as some other observation-based analyses. According to the lead-lag correlation between the QBO index (i.e., monthly zonal wind anomalies at 30 hPa over Singapore) and the NINO3.4 index, the relationship between the QBO and tropical SSTA went through a change around 1978–1980, and again in 1993–1995. During 1966–1974, the negative correlation between the QBO

and NINO3.4 indices reaches its maximum when the NINO3.4 index lags the QBO by less than 6 months. Correspondingly, positive correlations are observed when the NINO3.4 index leads the QBO by about 11–13 months or lags by about 12–18 months. However, the maximum negative correlations shifted from the NINO3.4 index lagging the QBO by about 0–6 months during 1966–1974 to by about 3–12 months during 1985–1992. This implies a delay in the connection of the QBO with the tropical tropospheric circulation and the Pacific SSTA after the late 1970s.

During 1975–1979, both the negative and positive correlations were relatively small and the QBO and ENSO were practically unrelated to each other, possibly reflecting the rapidly changing relationship. The phase-based life cycle composites confirm that, on average, there is a two-phase (6–7 months) delay in the evolution of the QBO associated anomalous Walker circulation, tropical SST, atmospheric stability, and tropospheric temperature anomalies during 1980–1994 in comparison with those in 1957–1978. This delay is likely associated with a more gradual extension of the QBO wind anomalies into the troposphere in the later period. Moreover, the interdecadal variations of the QBO associated vertical temperature anomalies in the troposphere and lower stratosphere and the atmospheric stability may also play a role in the difference of the QBO effects on the western Pacific deep convection. The interdecadal variation of the association between the QBO and tropospheric climate in the tropical Pacific may be largely due to the characteristic change of ENSO. The irregularity of the QBO may play a secondary role in the interdecadal variation of the association.

Besides the phase dependence of the association between the QBO and ENSO and the definition dependence of the QBO, the interdecadal change of the association may be another reason resulting in differing conclusions reached in previous investigations between the QBO and ENSO (Quiroz 1983; Maruyama and Tsuneoka 1988; Yasunari 1989; Barnett 1991; Angell 1992; Xu 1992). It will be interesting to further analyze the causes of the interdecadal shift of the relationship between the QBO and tropical SSTA.

In spite of possible physical reasons for the associations of the QBO and tropospheric climate and its interdecadal change, some non-physical factors may also be involved. For example, statistically, two oscillatory time series with close characteristic periods may generate some significant lead and lag correlations no matter whether they are physically linked or not. Thus, it is reasonable to suspect the physical reliability of the statistical connection between the QBO and ENSO, because they have close characteristic periods. However, the physical consistency among different variables in the connection between the QBO and

tropospheric circulation and their interdecadal change analyzed in this work and in HHKWK support the physical reality of the connection. Moreover, it is necessary to make clear that our work only suggests that a QBO cycle associated different zonal wind and thermal structure in its different phases can affect the evolution of tropospheric variability and the SST anomalies in the tropical Pacific through affecting the atmospheric stability and the Walker circulation in the tropical Pacific. It is also clear that the QBO cannot be a major forcing of a cold or warm ENSO event. However, the composite analysis suggests that the stratospheric may be connected with the atmospheric stability in the central and western Pacific at certain QBO phases that affects the SST anomalies in the equatorial Pacific. The effectiveness of the QBO effects on SST also depends upon the evolution within the troposphere. The shift of the QBO-ENSO relation actually reflects the effects of the tropospheric variations.

Another possible non-physical factor is the impact of observation system changes on the consistency of the datasets. For example, Pawson and Fiorino (1999), Randel et al. (2000), and Huesmann and Hitchman (2001, 2003) documented unrealistic interdecadal changes in the structure of the QBO and annual mean fields in the tropical stratosphere during 1958–2001 in the NCEP/NCAR reanalysis. A sudden temperature increase occurred around 1978, with an equatorial maximum of 3° K at 10 hPa near the tropopause. While the QBO in zonal wind is similar in both the 1958–1978 and 1979–2001 periods, the QBO in temperature is significantly reduced in amplitude and latitudinally contracted after 1978, and the QBO meridional circulation was stronger. Vertical temperature variations in the annual mean and QBO have been underestimated since the introduction of satellites. It is likely that the unrealistic jump was due to the inclusion of satellite data since 1979 in the NCEP/NCAR reanalysis data assimilation system (Pawson and Fiorino 1999; Huesmann and Hitchman 2003). Kinter et al. (2004) further suggested that the interdecadal shift in the 1970s in the NCEP/NCAR reanalysis products may be artifacts of changes in the observing system and/or the data assimilation procedures. However, the consistency of the results between using the ERA40 and NCEP/NCAR reanalyses may provide support for the physical reality of the interdecadal variation of the connection between the QBO and the tropical SSTA.

Acknowledgments Thanks go to James M. Wallace, Shuntai Zhou, Amy Butler, Michelle L'Heureux, Cristiana Stan, Xiaosong Yang, and Jian Lu for their useful discussion and suggestions. This work was supported by the NOAA CVP Program (NA07OAR4310310) (Hu and Huang), as well as NSF ATM-0830062 (Huang and Kinter), NSF ATM-0830068, NOAA NA09OAR4310058, NASA NNX09AN50G (Hu, Huang, and Kinter), and NSF ATM-0917743 (Wu).

References

- An S-I, Wang B (2000) Interdecadal change of the structure of the ENSO mode and its impact on the ENSO frequency. *J Clim* 13:2044–2055
- Angell JK (1992) Evidence of a relation between El Niño and QBO, and for an El Niño in 1991–92. *Geophys Res Lett* 19:285–288
- Barnett TP (1991) The interaction of multiple time scales in the tropical climate system. *J Clim* 4:269–285
- Gottelman A, Forster PMF (2002) A climatology of the tropical tropopause layer. *J Meteor Soc Jpn* 80(4):911–924
- Gray WM, Sheaffer JD, Knaff JA (1992a) Hypothesized mechanism for stratospheric QBO influence on ENSO variability. *Geophys Res Lett* 19:107–110
- Gray WM, Sheaffer JD, Knaff JA (1992b) Influence of the stratospheric QBO on ENSO variability. *J Meteor Soc Jpn* 70:975–995
- Holton JR, Tan T-C (1980) The influence of the equatorial quasi-biennial oscillation on the global circulation at 50 mb. *J Atmos Sci* 37:2200–2208
- Huang B, Hu Z-Z, Kinter III JL, Wu Z, Kumar A (2011) Connection of the stratospheric QBO with global atmospheric general circulation and tropical SST. Part I: methodology and composite life cycle. *Clim Dyn* (submitted)
- Huesmann A, Hitchman MH (2001) The stratospheric quasi-biennial oscillation in the NCEP reanalyses: Climatological structures. *J Geophys Res* 106:11, 859–11, 870
- Huesmann A, Hitchman MH (2003) The 1978 shift in the NCEP reanalysis stratospheric quasi-biennial oscillation. *Geophys Res Lett* 30:1048. doi:10.1029/2002GL016323
- Jin F-F, Hu Z-Z, Latif M, Bengtsson L, Roeckner E (2001) Dynamics and cloud-radiation feedbacks in El Niño and greenhouse warming. *Geophys Res Lett* 28(8):1539–1542
- Kessler WS, Kleeman R (2000) Rectification of the Madden-Julian oscillation into the ENSO cycle. *J Clim* 13:3560–3575
- Kinter JL III, Fennessy MJ, Krishnamurthy V, Marx L (2004) An evaluation of the apparent interdecadal shift in tropical divergent circulation in the NCEP-NCAR reanalysis. *J Clim* 17:349–361
- Maruyama T, Tsuneoka Y (1988) Anomalously short duration of the easterly wind phase of the QBO at 50 hPa in 1987 and its relationship to an El Niño event. *J Meteor Soc Jpn* 66:629–634
- Meehl GA, Washington WM (1996) El Niño-like climate change in a model with increased atmospheric CO₂ concentrations. *Nature* 382:56–60
- Nitta T, Yamada S (1989) Recent warming of tropical sea surface temperature and its relationship to the Northern Hemisphere circulation. *J Meteor Soc Jpn* 67:375–383
- Pawson S, Fiorino M (1999) A comparison of reanalyses in the tropical stratosphere, part 3: inclusion of the pre-satellite data era. *Clim Dyn* 15:241–250
- Quiroz RS (1983) Relationships among the stratospheric and tropospheric zonal flows and the southern oscillation. *Mon Wea Rev* 111:143–154
- Randel WJ, Wu F, Gaffen DJ (2000) Interannual variability of the tropical tropopause derived from radiosonde data and NCEP reanalyses. *J Geophys Res* 105:15509–15523
- Taguchi M (2010) Observed connection of the stratospheric quasi-biennial oscillation with El Niño–Southern oscillation in radiosonde data. *J Geophys Res* 115:D18120. doi:10.1029/2010JD014325
- Timmermann A, Latif M, Bacher A, Oberhuber J, Roeckner E (1999) Increased El Niño frequency in a climate model forced by future greenhouse warming. *Nature* 398:694–696
- Trenberth KE, Hurrell JW (1994) Decadal atmosphere–ocean variation in the Pacific. *Clim Dyn* 9:303–319
- Wallace JM, Panetta L, Estberg J (1993) A phase-space representation of the equatorial-stratospheric Quasi-Biennial oscillation. *J Atmos Sci* 50:1751–1762
- Wang B (1995) Interdecadal changes in El Niño onset in the last four decades. *J Clim* 8:258–267
- Wang R, Fraedrich K, Pawson S (1995) Phase-space characteristics of the tropical Stratospheric Quasi-biennial oscillation. *J Atmos Sci* 52(24):4482–4500
- Xu J-S (1992) On the relationship between the stratospheric quasi-biennial oscillation and the tropospheric southern oscillation. *J Atmos Sci* 49:725–734
- Yasunari T (1989) A possible link of the QBOs between the stratosphere, troposphere and sea surface temperature in the tropics. *J Meteor Soc Jpn* 67:483–493